AFFINITY OF RED BLOOD CELL MEMBRANE FOR PARTICLE SURFACES MEASURED BY THE EXTENT OF PARTICLE ENCAPSULATION

EVAN EVANS AND KAREN BUXBAUM, *Department of Biomedical Engineering, Duke University, Durham, North Carolina 27706 U.S.A.*

ABSTRACT An experimental technique and a simple analysis are presented that can be used to quantitate the affinity of red blood cell membrane for surfaces of small beads or microsomal particles up to 3 μm Diam. The technique is demonstrated with an example of dextran-mediated adhesion of small spherical red cell fragments to normal red blood cells. Cells and particles are positioned for contact by manipulation with glass micropipets. The mechanical equilibrium of the adhesive contact is represented by the variational expression that the decrease in interfacial free energy due to a virtual increase in contact area is balanced by the increase in elastic energy of the membrane due to virtual deformation. The surface affinity is the reduction in free energy per unit area of the interface associated with the formation of adhesive contact. From numerical computations of equilibrium configurations, the surface affinity is derived as a function of the fractional extent of particle encapsulation. The range of surface affinities for which the results are applicable is increased over previous techniques to several times the value of the elastic shear modulus. It is shown that bending rigidity of the membrane has little effect on the analytical results for particles 1–3 μm Diam and that results are essentially the same for both cup- and disk-shaped red cells. A simple analytical model is shown to give a good approximation for surface affinity (normalized by the elastic shear modulus) as a function of the fractional extent of particle encapsulation. The model predicts that a particle would be almost completely vacuolized for surface affinities $\gtrsim 10$ times the elastic shear modulus. Based on an elastic shear modulus of 6.6×10^{-3} dyn/cm, the range for the red cell-particle surface affinity as measured by this technique is from $\sim 7 \times 10^{-4}$ to 7×10^{-2} erg/cm^2. Also, an approximate relation is derived for the level of surface affinity necessary to produce particle vacuolization by a phospholipid bilayer surface which possesses bending rigidity and a fixed tension.

INTRODUCTION

The natural tendency of cells to aggregate is represented by the surface-to-surface affinity. The affinity is the reduction in free energy per unit area which is associated with the initial formation of adhesive contact. In general, the surface affinity may be much smaller than the work per unit area required to separate the surfaces. The strength of adhesion may involve subsequent chemical reactions (formation of bonds) between surface molecules; also, the work to separate the surfaces may include strong time-dependent, dissipative contributions. Consequently, to measure surface affinity, the equilibrium state of an adhesive contact must

---

The authors' present address is Department of Pathology, University of British Columbia, 2211 Wesbrook Mall, Vancouver, B.C. Canada V6T 1W5.

be observed. At equilibrium, the potential (virtual) decrease in free energy due to a virtual increase in contact area is just balanced against the potential increase in elastic energy due to the virtual deformation of the cell membrane and interior contents. Thus, if the elastic properties of these materials are known, mechanical analysis of deformation near the equilibrium configuration can be used to calculate the surface affinity. In other words, the elastic deformation of the cellular body produced by the formation of an adhesive contact is a "transducer" for the surface affinity. Based on this concept, Evans (1980) introduced an experimental procedure and method of analysis to measure the affinity of red blood cell membrane for other surfaces. Likewise, Skalak et al. (1977) used elastic deformations of a red cell to analyze the mechanics of red cell rouleau formation. Unfortunately, these previous methods required complicated numerical computations of minimum energy shapes for each specific red cell geometry and experimental situation. In addition, the range of surface affinities for which these methods were useful was limited to a fraction of the red cell membrane elastic shear modulus (i.e., $<7 \times 10^{-3}$ dyn/cm or erg/cm^2) because of the size and shape of the surface contact relative to the red cell area and volume. In this paper, we will present an experimental technique and simple analysis that can be used to determine the affinity of red cell membrane for surfaces of small beads or microsomal particles up to 3 μm Diam. We will show that the red cell geometry is not a factor in this case and that the range of surface affinities for which the analysis is applicable is increased to several times the value of the elastic shear modulus. In the next section, we will demonstrate the technique with an example of dextran-mediated adhesion of small, spherical, red cell fragments to normal red cells. The analysis that follows will show that the surface affinity is a simple function of the extent to which the particle is encapsulated, i.e., vacuolized, by the red cell membrane. The approach can be used to study the red cell membrane affinity for artificial material surfaces, surfaces complexed with lectins and other multivalent ligands, bacteria and other microsomes.

EXPERIMENTAL TECHNIQUE

First, small, nearly spherical fragments of human red blood cells are produced by heating a red cell suspension to temperatures above 48°C, where the particles spontaneously bud from the red cell; each fragment is a membrane-bound vesicle. These fragments are used as "test particles" which are added to a suspension of fresh red cells. A red cell is gently held by one suction micropipet; a red cell "particle" is selected with another micropipet and positioned adjacent to the flaccid red cell surface. Adhesion occurs after the release of the particle (Fig. 1). For the example shown in Fig. 1, the cells and particles are suspended in a solution which contains up to a few gram percent of dextran (either 70,000 or 150,000 mol wt). The micromanipulation procedure is like that described previously (Evans, 1980). Slightly cupped red cells are used so that the extent of encapsulation can be observed more easily. It will be shown that the shape of the red cell (i.e., cup or disk) does not significantly affect the result. Fig. 1 shows the difference between weak and strong surface affinities for two different concentrations of the same molecular weight dextran (1 and 3 g% of 70,000 mol wt) and for a higher molecular weight (3 g% of 150,000 mol wt). Details of these experiments are forthcoming.[1]

[1]Buxbaum, K. L., E. A. Evans, and D. E. Brooks. Manuscript in preparation.

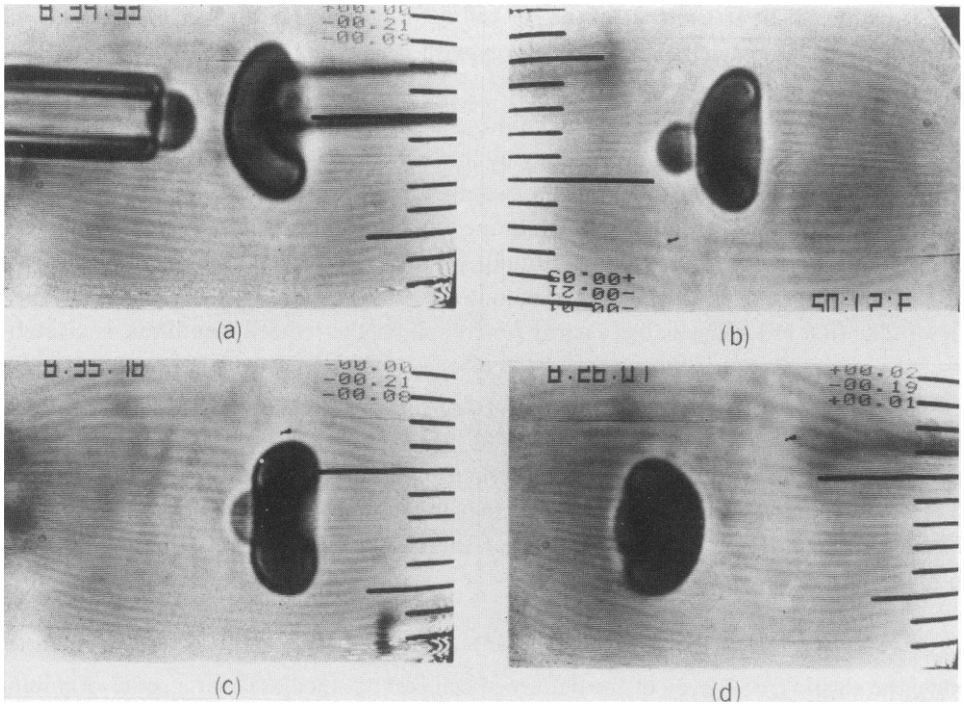

FIGURE 1 Videorecordings of cup-shaped red blood cells and spherical fragments of red blood cells. The sequence illustrates the technique for measurement of surface affinity: (*a*) the spherical "particle" is manipulated into position adjacent to the flaccid red cell surface; (*b–d*) are weak, moderate, and strong states of adhesion at mechanical equilibrium in different dextran solutions. *b* shows weak affinity in 1 g% dextran (70,000 mol wt); (*c*) moderate affinity in 3 g% (70,000 mol wt); and (*d*) strong affinity in 3 g% dextran (150,000 mol wt). Based on subsequent analysis and the value of 6.6×10^{-3} dyn/cm for the red cell membrane elastic shear modulus, the range of surface affinity is from 1×10^{-3} to 2×10^{-2} ergs/cm^2 for states *b–d*.

VARIATIONAL ANALYSIS OF PARTICLE ENCAPSULATION BY A RED BLOOD CELL

Because the particle and cell do not change volume and are free from external forces, there is no work done in the adhesion process near the equilibrium state. (The details of the attractive forces and molecular interactions between the surfaces in the contact region are cumulated into the free energy reduction of the interface, i.e., the surface affinity.) Hence, equilibrium is established when the variation in elastic free energy of the red cell deformation is equal to the variation in free energy of formation of the interfacial contact. If the adhesion process is uniform, the free energy variation for formation of the contact is given by the surface affinity, γ, times the variation in contact area, δA_c. Thus, equilibrium is expressed by,

$$\delta F_D = \gamma \, \delta A_c, \tag{1}$$

or equivalently,

$$\gamma = \mathrm{d}F_D/\mathrm{d}A_c, \tag{2}$$

where F_D is the elastic free energy of the red cell deformation. The surface affinity is equal to the derivative of the red cell elastic free energy with respect to the increase in contact area at equilibrium.

Since the interior of the red cell is liquid, the elastic free energy change produced by cellular deformation is contributed entirely by the membrane. For deformations of nonspherical red cells, the membrane behaves as a two-dimensionally incompressible material, i.e., it deforms at constant surface area by membrane extension (shear) and curvature change. As such, the membrane elasticity can be simply characterized by a shear modulus, μ, and a bending modulus, B (see Evans and Hochmuth [1978], or Evans and Skalak [1980], for review). The first order elastic free energy functional for the red cell membrane is given by,

$$F_D = \frac{\mu}{2}\int (\lambda^2 + \lambda^{-2} - 2)\, dA + \frac{B}{2}\int (K_1 + K_2)^2 dA, \tag{3}$$

where λ is the principal extension ratio for surface extension at constant area (illustrated later in Fig. 5); K_1 and K_2 are changes in principal membrane curvatures that result from the deformation. From Eq. 1, it is apparent that the elastic free energy of the membrane is a minimum for a fixed contact area, i.e.,

$$(\delta F_D)_{A_c} = 0.$$

Hence, the elastic free energy of the deformed cell can be calculated for a series of minimum energy states to give a function of the contact area. The surface affinity appropriate to each equilibrium configuration is the derivative of this function, F_D, with respect to contact area, i.e., Eq. 2.

The computational procedure for obtaining a minimum energy contour is implemented with an algorithm based on the Newton-Raphson technique of successive approximations to a set of geometric parameters which specify the curvilinear coordinates of the cell cross section (Evans, 1980); the algorithm is presently restricted to axisymmetric problems. This general approach requires that the initial cell geometry be given as well as the membrane elastic properties. Figs. 2 and 3 show the results of two computational models of the particle encapsulation; the particle is assumed to be rigid and spherical (other axisymmetric shapes can also be used). Fig. 2 shows the initial cell cross section as a normal biconcave disk shape with the progressive states of encapsulation *a*, *b*, and *c* on the dimple region. By comparison, Fig. 3 shows the initial cell cross section as a cup shape with the encapsulation *a*, *b*, and *c* on the convex face. (The cup shape in Fig. 3 was produced from the biconcave disk shape in Fig. 2 by an "induced moment" which acts to decrease the mean curvature of the cell, as do cupping agents [Evans, 1974; Evans, 1980]. The volume of the cup shape in Fig. 3 is 12% larger than the disk shape in Fig. 2 to match to the experimental example shown in Fig. 1.) The encapsulation results group into two categories determined by the fixed surface area and volume of the red cell in relation to the size of the particle. For sufficiently small particles, total encapsulation is possible without an increase in cell membrane area or decrease in cell volume, which would require energy changes several orders of magnitude greater than the elastic deformation of the flaccid cell. If the particle is too large, it can only be partially encapsulated; the pressure inside the cell and membrane tensions increase asymptotically as the limit of the geometric constraint is approached. The initial red cell disk shape used for Fig.

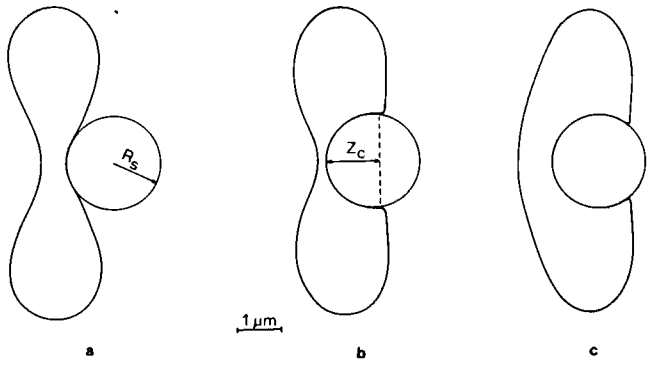

FIGURE 2 Minimum energy contours computed for progressive states of encapsulation of a rigid sphere by a disk-shaped red cell. The initial disk shape is the average cross section obtained by Evans and Fung (1972), represented by 135 μm^2 surface area and 94 μm^3 volume; the scale for 1 μm is illustrated above. The extent of encapsulation is given by the ratio of the contact distance, Z_c, divided by the sphere diameter, $2R_s$. The elasticity of the red cell membrane for these calculations is characterized by a bending to shear rigidity ratio of 10^{-2}.

2 represents the normal values of surface area (~135 μm^2) and volume (~94 μm^3) measured for red cells in isotonic media (Evans and Fung, 1972). With these values for surface area and volume, particle sizes of $\lesssim 3$ μm can be completely encapsulated by the red cell.

The effect of relative size is illustrated in Fig. 4, which shows the calculated rate of increase in membrane elastic energy of the disk-shaped cell with increase in contact area, i.e., the surface affinity required to produce a specific equilibrium contact area. The dashed curves represent the results for all particles with diameters of 1 to 3 μm; the dotted curve is the result for a specific particle diameter of 5 μm which illustrates the geometric limitation for particle sizes >3 μm. The "transducer" feature of the elastic membrane deformation is apparent from Fig. 4, where Eqs. 2 and 3 have been scaled to be dimensionless and the surface affinity is scaled by the membrane elastic shear modulus.

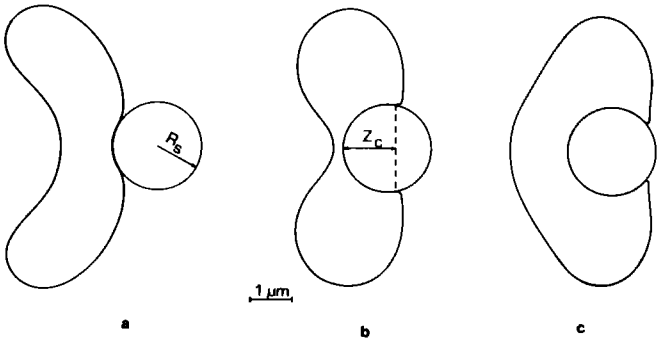

FIGURE 3 Minimum energy contours computed for progressive states of encapsulation of a rigid sphere by a cup-shaped red cell. The initial cup shape was produced from the biconcave disk in Fig. 2 by an "induced surface moment" which decreases the mean curvature of the cell, as do cupping agents. The volume of the cup shape is 12% larger than the disk in Fig. 2 to represent the experimental example shown in Fig. 1. The bending to shear rigidity ratio of the membrane is modeled by the same value as for Fig. 2.

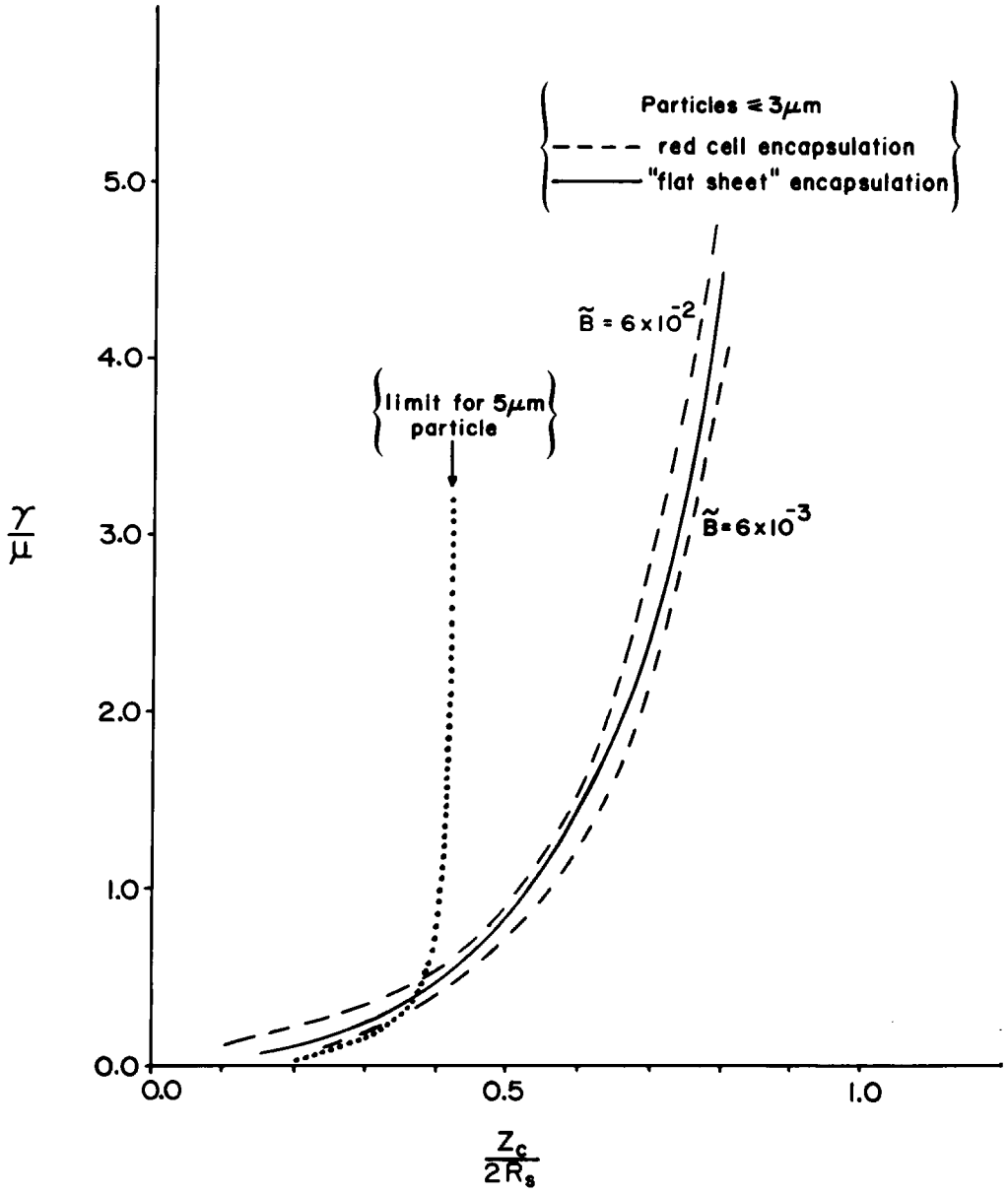

FIGURE 4 The free energy reduction per unit area in formation of adhesive contact, i.e., the surface affinity, γ, normalized by the membrane elastic shear modulus, μ, versus the fractional extent of encapsulation, $Z_c/2R_s$. The dimensionless surface affinity is the rate of increase of the membrane elastic free energy with respect to increase in contact area, derived from a series of equilibrium (minimum energy) states like those illustrated in Figs. 2 and 3. The dashed curves are the results for particles in the range of 1 to 3 μm Diam; the size is represented by the bending to shear rigidity ratios of 6×10^{-2} and 6×10^{-3}, respectively. For particle sizes larger than 3 μm (e.g., 5 μm), the fixed surface area and volume of the red cell limit the extent of encapsulation, as shown by the dotted curve. The solid curve is the simple result for encapsulation of a particle by an infinite, flat, elastic membrane surface.

The other important factor in the membrane compliance is the ratio of bending to shear rigidity given by $\tilde{B} = B/\mu R_s^2$. Based on previous analysis of the effect of bending versus shear rigidity on micropipet aspiration of red cells (Evans, 1980), the upper bound for the membrane bending modulus appears to be on the order of $B = 10^{-12}$ dyn-cm (erg). For particle diameters in the range of 1 to 3 μm, the bending to shear rigidity ratio varies between 6×10^{-2} and 6×10^{-3}; the dashed curves represent these rigidity limits. Clearly, the bending rigidity of the membrane has little effect on the results for particle diameters on the order of a micrometer. The normalized surface affinity depends on the fractional extent of encapsulation of the particle, $Z_c/2R_s$. For particles that can be completely encapsulated, the surface affinity versus extent of encapsulation depends only slightly on the bending to shear rigidity ratio (shown as the dashed curves in Fig. 4; see Appendix I for the effect of bending rigidity on the equilibrium shape). The results are essentially the same for both the cup and disk shape geometries. (If the dimple opposite the encapsulation is forced to "pop out," the derivative of the elastic energy is slightly higher than the dashed curves local to this state, e.g., between Fig. 2 *b* and *c* or Fig. 3 *b* and *c*.) The results for encapsulation of small particles are essentially independent of particle size, because the elastic free energy per unit membrane area decreases with the inverse of the square of the radial distance from the contact region. Thus, for a membrane contour where the initial curvature is much less than the particle curvature, the deformation in the vicinity of the contact region is like that produced in a "flat" surface and can be calculated analytically. This feature provides the basis for a simple model of the encapsulation process.

PARTICLE ENCAPSULATION BY A "FLAT" ELASTIC MEMBRANE

The simple model for particle encapsulation by a flat membrane surface is illustrated schematically in Fig. 5. In this simple model, we will neglect the bending rigidity of the sheet and assume that the membrane makes a sharp bend at the edge of the contact region. (For bending to shear rigidity ratios $<6 \times 10^{-2}$, the assumption is reasonable, as is evident in Figs. 2–4.) The deformation must be analyzed throughout the entire membrane surface and then used with Eqs. 2 and 3 to determine the surface affinity that is associated with an equilibrium extent of encapsulation. The dashed lines in Fig. 5 outline the initial (undeformed) geometry of the surface and a differential surface element; the solid lines represent the corresponding material regions in the deformed state. Since the membrane material is two-dimensionally incompressible, the initial and deformed elements of the surface have the same area; therefore, the deformation is characterized by a single extension ratio. The extension ratio is given by the ratio of the differential length of the element along the meridian in the deformed state to that in the initial state. For example, the extension ratio for the deformation of the differential element shown in Fig. 5 is given equivalently by either $\lambda = dr/dr_0$ or $\lambda = r_0/r$. By equating areas integrated from the symmetry axis outward in the initial and deformed surfaces, we obtain analytical expressions for the extension ratio squared for any location on the spherical contact region and in the outer surface. The extension ratio squared increases from a value of unity at the axis of symmetry to a maximum at the edge of the contact region and then decreases inversely with the radius squared in the outer region to a value of unity at large distances from the origin. Analytical expressions may be derived for the extension ratio

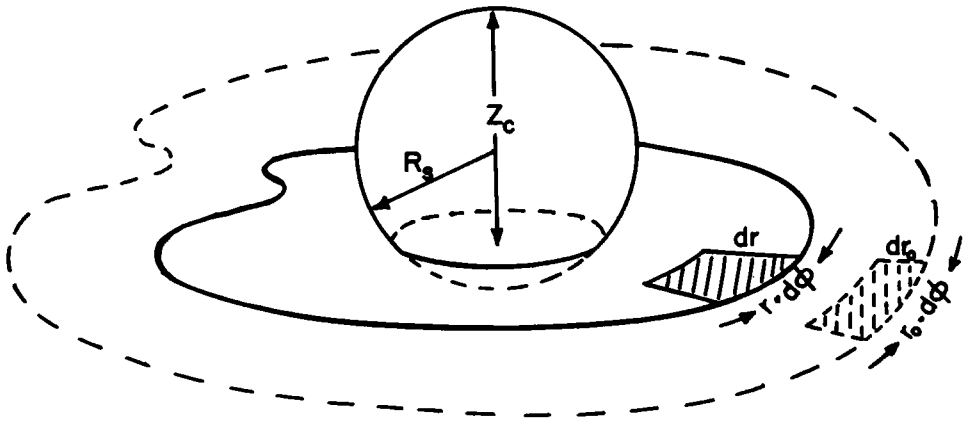

FIGURE 5 Schematic illustration of encapsulation of a spherical particle by a flat, elastic membrane surface. The dashed lines represent the undeformed geometry of the surface; the solid lines represent the corresponding material regions in the deformed state, where the deformation maintains constant surface area (i.e., the surface is two-dimensionally incompressible). As such, the deformation is characterized by a single extension ratio for stretch along the meridional direction.

squared in terms of the membrane area which lies within a circle defined by the meridional position. Over the contact region, the extension ratio squared is given by,

$$\lambda^2 = 1/(1 - A/4\pi R_s^2), (A \leq A_c) \tag{4}$$

and in the flat surface exterior to the contact, the expression is,

$$\lambda^2 = A/(A - A_c^2/4\pi R_s^2), (A \geq A_c). \tag{5}$$

Now that the deformation field is specified, the elastic free energy, Eq. 3, can be integrated; the upper limit for the integration is the total area of the membrane surface, A_T. A simple closed form for the elastic free energy is obtained by integration of Eq. 3 with the expressions for the extension ratio,

$$F_D = (2\pi R_s^2)\mu\,[-(1 + x^2)\ln(1 - x) - x(1 + x/2) + x^2 \ln(1 - x^2/\tilde{A})], \tag{6}$$

where the fractional extent of encapsulation is defined by $x = Z_c/2R_s$ or $A_c/4\pi R_s^2$. $\tilde{A}$ is the ratio of the membrane area to the particle surface area, i.e., $\tilde{A} = A_T/4\pi R_s^2$. The surface affinity is obtained from the derivative of the elastic free energy with respect to the contact area; therefore,

$$\gamma/\mu = [x^2/(1 - x) - x\ln(1 - x) + x\ln(1 - x^2/\tilde{A}) - x^3/(\tilde{A} - x^2)]. \tag{7}$$

An estimate of the bending energy contribution to the equilibrium relation for surface affinity, Eq. 7, is derived in Appendix II; the result is (Eq. A9),

$$\frac{1}{\mu}\frac{dF_B}{dA_c} \sim 2\tilde{B} + \sqrt{2\tilde{B}}\left[1 + \frac{1}{2}x(1 - x)^{-1/2} - (1 - x)^{1/2}\right],$$

where F_B is the approximation to the bending energy. The bending rigidity establishes a threshold for the minimum surface affinity necessary for adhesion to occur, i.e.,

$$\frac{\gamma}{\mu} > 2\tilde{B},$$

which is obtained from the limit as $x \rightarrow 0$. Here, the bending to shear rigidity ratio, $\tilde{B}$, is an initial threshold which establishes the minimum surface affinity necessary for adhesion to occur. This bias is also observed in the numerical results for encapsulation by the red blood cell given in Fig. 4 as the dashed curves; as before, the bending rigidity offers little resistance to the deformation. For membrane surface areas that exceed twice the particle surface area, the effect of the finite extent of the membrane may be neglected and the last two terms inside the brackets may be omitted in Eq. 7. With this simplification, Eq. 7 is plotted in Fig. 4 as the solid curve for a bending to shear rigidity ratio of zero. Comparison of the solid curve with the dashed curves in Fig. 4 clearly demonstrates that the simple analysis is a good approximation. Thus, if the elastic shear modulus of the red cell membrane is known, observation of the extent of encapsulation provides a measure for the surface affinity between the cell membrane and particle surface. A similar relation is derived in Appendix II for the encapsulation of a particle by a bilayer membrane surface which has no shear rigidity (Eq. A8).

CONCLUSIONS

For small particles (typically 3 μm or less in diameter), the extent of encapsulation by a flaccid red blood cell membrane can be used to quantitate the affinity of the membrane for the particle surface. In addition, a simple analytical model gives a good approximation for the surface affinity normalized by the membrane elastic shear modulus as a function of the fractional extent of particle encapsulation. For larger particles, the surface area and volume constraints established by the red cell ultimately restrict the encapsulation of the particle and compromise the correlation of the extent of encapsulation with the surface affinity.

As is evident from the theoretical result, Eq. 7, total encapsulation of a small particle would require an infinitely large surface affinity. In actuality, the membrane would first reach its elastic limit and then yield. The red cell membrane appears to yield when the maximum extension ratio exceeds 3 or 4:1 (Evans and Hochmuth, 1978). Therefore, from Eqs. 4 and 7, we would expect the particle to be vacuolized for surface affinities $\gtrsim$ten times the elastic shear modulus. The normal value for the membrane elastic shear modulus of human red cells at 25°C is 6.6×10^{-3} dyn/cm or erg/cm^2 (Waugh and Evans, 1979); hence, the upper limit for the surface affinity as measured by this method is $\sim 7 \times 10^{-2}$ erg/cm^2. Also, vacuolization of a particle by a phospholipid bilayer membrane would occur for surface affinities greater than a value determined by the bending rigidity and the isotropic tension supported by the bilayer (see Eq. A8 in Appendix II).

We thank Dr. D. E. Brooks, Department of Pathology, University of British Columbia, Vancouver, B.C. for his dextran contributions and helpful insight.

This work was supported by National Institutes of Health grant HL16711.

Received for publication 2 October 1980 and in revised form 20 December 1980.

APPENDIX I

The rate of change of membrane elastic free energy with change in contact area is not greatly affected by bending to shear rigidity ratios <0.1 (Fig. 4). However, the equilibrium shape of the red cell for a given extent of particle encapsulation is affected by this ratio. For example, Fig. A1 shows the equilibrium shapes of the red cell computed for a three order of magnitude range of the bending modulus and a fixed extent of encapsulation of a 3 μm particle. Little effect on the shape is observed until the bending to shear rigidity ratio exceeds 10^{-2} (which corresponds to a bending modulus of 10^{12} dyn-cm). The shapes in Fig. A1 suggest that electron microscopy of fixed samples (perhaps even scanning electron microscopy) could provide measurements or estimates of the membrane curvature adjacent to the contact region. In turn, knowledge of the curvature could be used to deduce the bending modulus of the membrane.

APPENDIX II

The explicit contribution of bending energy to the variation of the total deformation energy with respect to contact area is shown in Fig. 4, as determined by numerical computation. Here, we will derive an approximate assessment of the bending energy contribution to the total elastic energy and to the surface affinity. To make this estimate, we assume that the membrane sheet can be partitioned into three regions: the exterior surface, which is flat; a localized bend at the edge of the contact region; and the spherical contact region. With this partition, the bending energy is approximated by,

$$F_B \sim \frac{B}{2}\left(\frac{4}{R_s^2}\right) A_c + \frac{B}{2}\int_e K_e^2 \, dA, \tag{A1}$$

where the first term is the bending energy for the spherical contact region and the second term approximates the bending energy of the localized bend between the exterior sheet and spherical contact region. In Eq. A1, we assume that the bend is relatively sharp so that only the principal curvature, K_e, in the meridional plane is important. Likewise, if the bend is sharp, the second term is approximated closely by,

$$\frac{B}{2}\int_e K_e^2 \, dA_e \simeq B\pi r_e \int_e K_e^2 \, ds, \tag{A2}$$

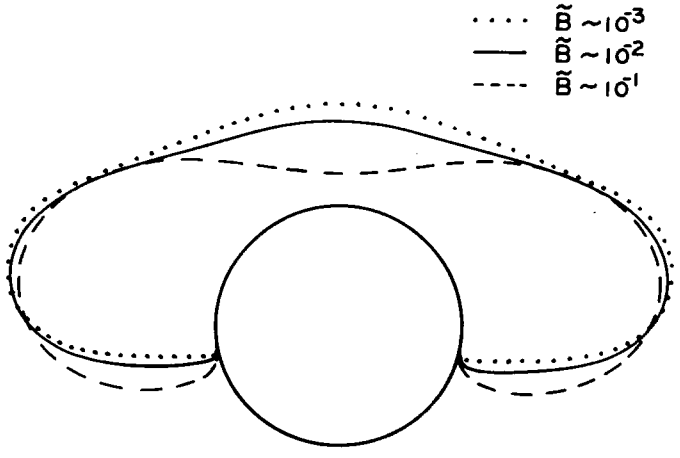

FIGURE A1 Equilibrium shapes of a red cell computed for a three order of magnitude range of bending rigidity.

where r_e is the circular radius of the annular bend, and ds is the differential length along the meridian which is the width dimension of the annular element. Using the variables defined in the text, we reduce Eq. A1 to,

$$F_B \sim 8\pi B \cdot x + 2\pi R_s B\sqrt{x - x^2} \int_e K_e^2 \, ds. \tag{A3}$$

The remaining task is to estimate the curvature, K_e, of the bend. With the equations of mechanical equilibrium for cylindrical bending (appropriate for the sharp bend), the principal membrane tension along the meridian is derived from the following equations (Evans and Skalak, 1980),

$$T_m \sin\theta = \cos\theta \cdot \frac{dM}{ds}$$

$$\frac{dT_m}{ds} + \frac{d\theta}{ds} \cdot \frac{dM}{ds} = 0,$$

where M is the bending moment, s is the curvilinear distance along the meridian, θ is the angle between the surface normal and the axis of symmetry, and T_m is the principal tension. The bending moment is proportional to the curvature,

$$M = B \cdot K_e,$$

and the curvature is,

$$K_e = \frac{d\theta}{ds}.$$

These equations combine to give a relation for the curvature as a function of the tension, T_m^0, in the outer sheet and the curvilinear angle, θ,

$$T_m = T_m^0 - \frac{B}{2} K_e^2,$$

$$T_m = T_m^0 \cos\theta,$$

hence,

$$|K_e| = \sqrt{\frac{2\,T_m^0}{B}}\sqrt{(1 - \cos\theta)}. \tag{A4}$$

The curvature varies with position in the bend; therefore, we must evaluate the integral in Eq. A3,

$$\int_e K_e^2 \, ds = \left| \int_e K_e \, d\theta \right|,$$

which will only depend on the value of the angle θ at the contact with the sphere. At this tangential location, the cosine is given by,

$$\cos\theta_c = (1 - 2x). \tag{A5}$$

Hence,

$$\sqrt{\frac{B}{2T_m^0}} \int_e K_e^2 \, ds = 2\sqrt{2}\,[1 - (1 - x)^{1/2}]. \tag{A6}$$

Using Eqs. A3, A4, and A6, we obtain an estimate of the bending energy,

$$F_B \sim 8\pi B \cdot x + B\pi R_s \sqrt{B \cdot T_m^0}\,[\sqrt{x - x^2} - (1 - x)\sqrt{x}]. \tag{A7}$$

To determine the contribution to the surface affinity relation, we take the derivative with respect to contact area of Eq. A7,

$$\frac{dF_B}{dA_c} = \frac{1}{4\pi R_s^2}\frac{dF_B}{dx}.$$

If the tension in the outer sheet is constant, the derivative of Eq. A6 leads to an approximation to the surface affinity relation for particle encapsulation by a membrane without shear rigidity and with a constant isotropic tension, $\bar{T}$ (e.g., a phospholipid bilayer membrane). We must include the work of displacement of the isotropic tension at the outer boundary of the sheet, $4\pi R_s^2\,\bar{T}\cdot x^2$. The surface affinity is obtained from the derivative with respect to contact area of this work plus the bending energy derivative,

$$\frac{\gamma}{\bar{T}} \sim 2(x + \tilde{B}) + \sqrt{\tilde{B}}f(x)/\sqrt{x - x^2}, \tag{A8}$$

where $\tilde{B} \sim B/(\bar{T}\cdot R_s^2)$, and the function $f(x)$ is,

$$f(x) \equiv [(1 - 2x) + 2x(1 - x)^{1/2} - (1 - x)^{3/2}].$$

(There is a maximum value, $\hat{\gamma}$, at some extent of encapsulation which depends on the membrane tension and bending rigidity; for surface affinities $>\hat{\gamma}$, the particle would be totally encapsulated.)

On the other hand, for the red cell membrane with shear rigidity, the tension in the outer sheet drops off inversely with the radial distance squared. The tension at the edge of the contact region is given approximately by (Evans and Skalak, 1980),

$$T_m^0 \sim \frac{\mu}{2}\frac{x}{(1 - x)}.$$

Therefore, the bending energy relation reduces to,

$$F_B \sim 8\pi B\cdot x + 4\sqrt{2}\,\pi R_s\sqrt{B\cdot\mu}\,[x - x(1 - x)^{1/2}].$$

This equation yields the following normalized contribution to the surface affinity relation, Eq. 7, in the text:

$$\frac{1}{\mu}\frac{dF_B}{dA_c} \sim 2\tilde{B} + \sqrt{2\tilde{B}}\left[1 + \frac{1}{2}x(1 - x)^{-1/2} - (1 - x)^{1/2}\right], \tag{A9}$$

where $\tilde{B} \equiv B/(\mu\cdot R_s^2)$.

REFERENCES

EVANS, E. A. 1974. Bending resistance and chemically induced moments in membrane bilayers. *Biophys. J.* **14**:923–931.

EVANS, E. A. 1980. Minimum energy analysis of membrane deformation applied to pipet aspiration and surface adhesion of red blood cells. *Biophys. J.* **30**:265–284.

EVANS, E., and Y. C. FUNG. 1972. Improved measurements of the erythrocyte geometry. *Microvasc. Res.* **4**:335–347.

EVANS, E. A., and R. M. HOCHMUTH. 1978. Mechano-chemical properties of membranes. *Curr. Top. Membr. Transp.* **10**:1–64.

EVANS, E. A., and R. SKALAK. 1980. Mechanics and Thermodynamics of Biomembranes. C.R.C. Press, Boca Raton, Fla.

SKALAK, R., P. R. ZARDA, K-M. JAN, and S. CHIEN. 1977. Theory of rouleau formation. *INSERM (Inst. Nat. Sante Rech. Med.) Euromech 92 Proc.* **71**:299–308.

WAUGH, R., and E. EVANS. 1979. Thermoelasticity of red blood cell membrane. *Biophys. J.* **26**:115–132.